

Reducing Out-of-Plane Deformation of Soft Robotic Actuators for Stable Grasping

Rob B.N. Scharff¹, Jun Wu^{*1}, Jo M.P. Geraedts¹ and Charlie C.L. Wang²

Abstract—For grasping (unknown) objects, soft pneumatic actuators are primarily designed to bend towards a specific direction. Due to the flexibility of material and structure, soft actuators are also prone to out-of-plane deformations including twisting and sideways bending, especially if the loading is asymmetric. In this paper, we demonstrate the negative effects of out-of-plane deformation on grasping. A structural design is proposed to reduce this type of deformation and thus improve grasping stability. Comparisons are first performed on soft pneumatic actuators with the same bending stiffness but different resistances to out-of-plane deformation, which is realized by changing the cross-section of the inextensible layer. To reduce out-of-plane deformation, a stiffening structure inspired by spatial flexures is integrated into the soft actuator. The integrated design is 3D printed using a single material. Physical experiments have been conducted to verify the improved grasping stability.

I. INTRODUCTION

One practical application of soft robots is to pick and place objects in unknown environments. In soft robots, the grasping motion is often realized by the bending of soft pneumatic actuators, induced by the inflation of air chambers that are made of soft material [1]–[4]. While the soft actuators are designed to bend towards a specific direction, their flexibility allows them to deform in other directions when the reaction force from the objects is asymmetric – i.e., not in the plane of intended bending. As illustrated in Fig. 1, out-of-plane deformations include sideways bending (B) and a combination of bending and twisting (C). This type of deformation is not typically observed either in our human hands or in conventional rigid robotic grippers [5]–[8]. Rigid robotic grippers and also human hands, composed of rigid phalanges connected by joints, have a limited number of degrees of freedom (DOFs). In contrast, soft pneumatic actuators have a large number of DOFs which allows complex deformation when they are confronted with different loading conditions. As soft actuators are intended to operate in situations where the shape and position of objects are unknown, the chance of having these asymmetric loadings is high.

Instability of soft grippers due to out-of-plane deformation was discussed at the early stage of soft robotics research [9]. Dexterous grasping using soft pneumatic actuators revealed significant out-of-plane deformations [10]. A sensorized version of the soft hand confirmed that significant twisting and

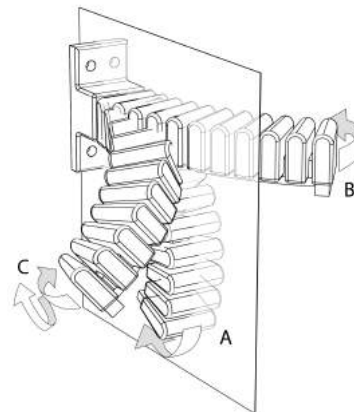


Fig. 1: Besides in-plane bending (A), the flexibility of soft pneumatic actuators allows out-of-plane deformations including sideways bending (B) and a combination of bending and twisting (C), which could reduce the stability of grasping.

lateral bending occur when grasping a spherical object [11]. In line with this, in Fig. 2 we demonstrate that a three-fingered soft pneumatic gripper failed to stably grasp a sphere due to the out-of-plane slippage of the actuators. Similar failure is also reported for a four-fingered gripper [9], [12].

The out-of-plane behavior is often not reported during evaluation of soft pneumatic actuators. For example, force measurements of soft pneumatic actuators are commonly performed using symmetric loadings [3], [13], [14]. Furthermore, optimization of the actuators commonly focuses only on the in-plane deformation [3], [15], neglecting the consequences of the design changes on the out-of-plane behavior of the actuator.

In early works spring models were developed to understand slipping phenomena of soft grippers [9], [16]. Morrow et al. [12] suggested the use of lower friction fingertips to prevent some out-of-plane slippage. This comes with a loss of desired in-plane friction as well. To reduce out-of-plane deformation, a simple way is to increase the stiffness by fabricating the actuators using stiffer materials. However, this also increases the in-plane stiffness and therefore requires a higher actuation effort. Anisotropic stiffnesses can be created using paper layers [3], or fiber reinforcements [17]. However, it is not known how these principles can be applied to reduce out-of-plane deformation. Different from existing works, we improve grasping stability by structural design that increases out-of-plane stiffness without modifying the in-plane stiffness.

¹ R.B.N. Scharff, J. Wu and J.M.P. Geraedts are with the Department of Design Engineering, Delft University of Technology, 2628 CE, The Netherlands.

² C.C.L. Wang is with the Department of Mechanical and Automation Engineering, The Chinese University of Hong Kong, Shatin, Hong Kong.

* Corresponding Author (E-mail: j.wu-1@tudelft.nl)

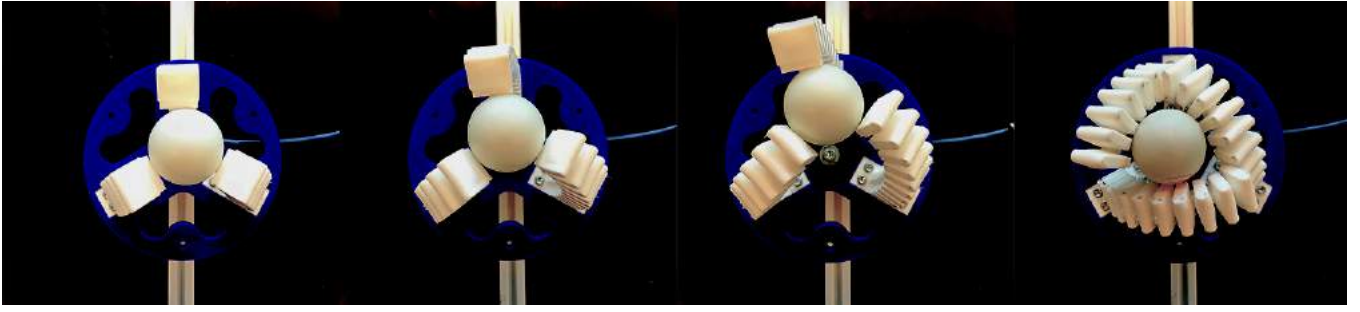


Fig. 2: A three-fingered soft pneumatic gripper failed to grasp a spherical object due to the progressive out-of-plane deformation. Slipping occurs at a pressurization of about 400 kPa.

A. Our approach

In this paper, we approach the problem of out-of-plane deformation by structural analysis. Our purpose is two-fold. First, we demonstrate the effects of out-of-plane deformation on the grasping stability of soft actuators (Section II). This demonstration, through the physical experiments and numerical simulations, is performed on a pair of actuators which have the same in-plane bending stiffness but different stiffnesses to out-of-plane deformation. We evaluate these actuators in terms of exerted forces when they bend towards a flat and an angled surface. This demonstration serves as a guideline for structural optimization of soft actuators.

Second, we propose a stiffening structure to increase the out-of-plane stiffness (Section III). This stiffener pattern has a marginal in-plane bending stiffness, but provides strong resistance to the out-of-plane deformation. Our design is inspired by the spatial flexures [18]–[20]. The improved actuator is fabricated by 3D printing using a single material, and is verified by physical experiments (Section IV).

II. OUT-OF-PLANE DEFORMATION

This section is dedicated to demonstrate and analyze the importance of the resistance to out-of-plane deformation for stable grasping. The out-of-plane slipping of soft pneumatic actuators includes the effects of sideways bending, twisting and twist-coupled bending. The influences of these deformations to the stability of grasping depend not only on the actuator design but also on the loading that is applied. Moreover, the actuator's stiffness with regards to these deformations changes over the actuation range. Analytical description of such complex deformation is difficult. Our approach thus mainly relies on physical experiments and numerical simulations.

To isolate the out-of-plane deformation from other factors, we test a pair of actuators which have an equal stiffness to in-plane bending, but with different stiffnesses to out-of-plane deformation. Building upon a commonly used type of soft actuators as the basis, an extra beam is added to its inextensible layer (see Fig. 3). The extra beam is placed along the full length of the actuator. For small in-plane deflections, the radius of curvature R of a beam is calculated by

$$R = \frac{EI_z}{M}, \quad (1)$$

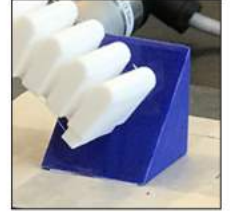
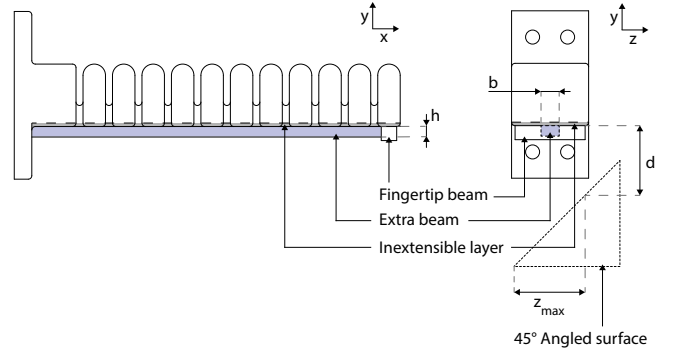


Fig. 3: Experimental setup. We measure the vertical component of the in-plane force for an actuator interacting with an object. In this scenario, the object has a 45° angled surface.

where E and M are Young's modulus and the applied bending moment, respectively [21]. I_z is the area moment of inertia around the z -axis,

$$I_z = \frac{bh^3}{12}, \quad (2)$$

where b indicates the base width and h indicates the height of the beam.

We compare two beams with different dimensions of the cross-section, one with a width $b = 20$ mm and a height $h = 2$ mm, and the other one with $6 \text{ mm} \times 3 (\approx \sqrt[3]{80/3})$ mm. The height is designed smaller than the width to prevent buckling on the beams. The area moment of inertia for in-plane bending, I_z , for these two beams is the same. In contrast, the area moment of inertia for sideways bending (I_y) has a difference of around 25 times – with the one having $b = 20$ mm being stiffer. This is calculated by switching

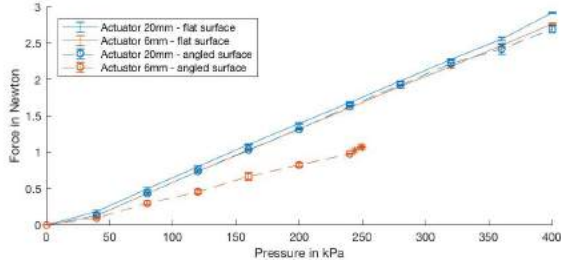


Fig. 4: Vertical component of the in-plane forces exerted by an actuator having a 6 mm beam (blue) or a 20 mm beam (orange). When confronted with a flat surface (symmetric loading), the exerted forces as represented by solid curves are nearly the same for both actuators. When confronted with an angled surface (asymmetric loading), the actuator with 20 mm beam exerts comparable forces (dashed, blue) as in the case of symmetric loading. In contrast, the actuator with 6 mm beam exhibits smaller forces (dashed, orange) and fails to consistently exert a force when the pressure is larger than 240 kPa.

b and h when considering another bending direction.

The torsional stiffness of the actuator is also changed when different beams are attached. The torsional stiffness k of a beam can be calculated by

$$k = \frac{J_T G}{l} \quad (3)$$

where l is the beam's length, G is the shear modulus and J_T is the torsional constant. When $b \geq h$, the torsional constant of a rectangular cross-section can be approximated by

$$J_T \approx bh^3 \left(\frac{1}{3} - 0.21 \frac{h}{b} \left(1 - \frac{h^4}{12b^4} \right) \right) \quad (4)$$

with an error not greater than 4% (ref. [21]). Therefore, the torsional stiffness of the 20 mm-width beam is around 35% higher, which is also good against the unwanted out-of-plane deformation.

To ensure identical contacts with the object in the presence of variably sized beams, we add a fingertip-beam along the z -axis to the free-end of the actuator. Both actuators are fabricated by a 3D printer using *Fused Deposition Modeling* (FDM). A flexible filament (Ultimaker TPU 95A) is used.

A. Experimental Analysis

To quantify the actuator's resistance to different deformations during grasping, we test the force exertion of the actuators on a flat surface (symmetric loading) and a surface under an angle of 45 degrees (asymmetric loading, cf setup in Fig. 3). The contact surfaces of both objects have been printed flat on the printbed to ensure identical friction coefficients. The distance (d) between the first contact and the tip of the actuator (i.e., the inextensible layer) is 20 mm. When the actuator is pressurized, it exerts a force to the flat (or inclined) surface. The vertical component of this force is recorded. We progressively increase the pressure by using 40 kPa pressure intervals. As the actuators show very

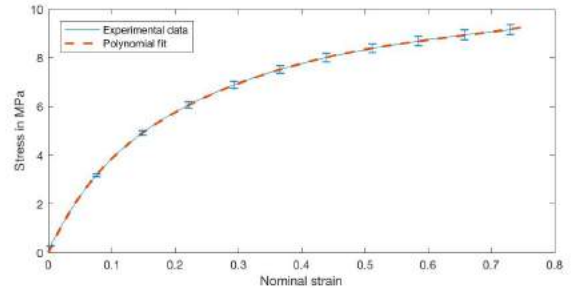


Fig. 5: Average stress-strain relationship for 10 TPU 95A dumbbells and fitted nonlinear material model.

slow slipping, we wait 10 seconds at each pressure before recording the corresponding force. When the actuator bends towards the inclined surface its free-end slips down along the surface. We consider the actuator as slipped away when its sideways displacement reaches 20 mm (z_{\max} , cf Fig. 3). Each actuator is tested three times. Here we purposely measure the contact interaction when the actuator is already in a bent configuration, as this more closely simulates a real grasping situation. The actuator's stiffness with respect to the out-of-plane deformations such as sideways bending and twisting usually decreases rapidly when the bending of the actuator is increased.

The experimental results are shown in Fig. 4. The solid curves represent the measured vertical forces under symmetric loadings. These two curves are very close. This confirms that the in-plane bending behavior of actuators with the same I_z (Eq.(2)) is almost identical. The dashed curves are corresponding to vertical forces when the actuators are confronted with an angled surface, i.e., an asymmetric loading condition. The actuator with a wider beam is still able to exert a large force. In contrast, the other actuator slipped away before the pressure reaches 250 kPa, and failed to apply a large force onto the angled surface. Slippage points are indicated with a star in Fig. 4. This comparison reveals the importance of the out-of-plane stiffness for grasping stability.

B. Numerical Simulation

We further verify the different behaviours in deformation by using numerical simulation.

First of all, the tensile properties of the material (Ultimaker TPU 95A) were determined from experiments. A total of 10 dumb-bell test pieces were 3D printed in different XY-orientations on the printbed. We used a test length of 25 mm and a test speed of 500 mm/min, according to the ISO 37 norm (test piece type 1). The (average) stress-strain relationship is plotted in Fig. 5. As the material behavior is nonlinear, a second order polynomial strain energy function was selected to fit the measured data. The friction coefficient was estimated through a sliding test. The slipping point of the Ultimaker TPU 95A surface on an angled surface of smooth PLA (all obstacle contact surfaces are printed flat on the buildplate) was determined at 25 degrees. Therefore, the static friction coefficient was determined at

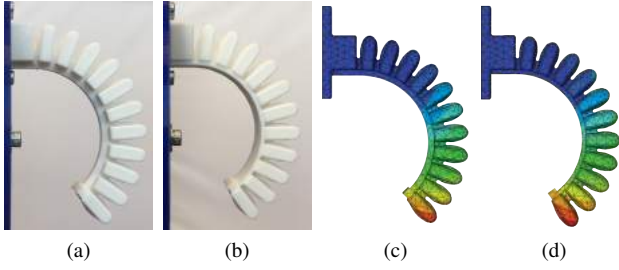


Fig. 6: The actuator with a 6 mm-width beam (a) and the actuator with a 20 mm-width beam (b) show almost identical bending behavior (demonstrated at a pressure of 400 kPa). The simulation results ((c) & (d)) agree with the physical experiments. The colors projected on the deformed actuators indicate the magnitude of the spatial displacement of the nodes, ranging between 0 mm (dark blue) and 120 mm (dark red) for all simulation results.

$\mu = \arctan(25^\circ) \approx 0.47$. The pressure is increased slowly in our experiments to assume the static friction holds.

Numerical simulations were performed using ABAQUS. The NLgeom option in ABAQUS is used to enable simulating large displacements. The actuator and the obstacle have been positioned in the same configuration as shown in Fig. 3. For the angled obstacle, we use a finite sliding formulation. For the flat obstacle, we use a small sliding formulation. We also include the effect of gravity on the actuator and detect self-contact between the bellows. After applying a pressure of 400 kPa to the actuators. We output the in-plane components of the forces due to the contact pressure and the frictional stress on the obstacle.

The simulation results are reported in Figs. 6-8. Fig. 6 confirms that the 6 mm beam actuator and 20 mm beam actuator exhibit the similar in-plane bending in the absence of obstacles. Fig. 7 (a) and (c) show that the actuators deform similarly when they are resisted by a flat surface. When they are confronted with an angled surface, the actuator with a 6 mm beam, Fig. 7(b), has a larger sideways deformation than the one with a 20 mm beam (d). The vertical contact forces in numerical simulations are plotted in Fig. 8. Similar to the physical test results plotted in Fig. 4, it shows that the actuator with the 6 mm beam failed to exert a larger force on the angled surface (dashed orange curve). Although the simulation of contact force on a flat surface is in good agreement with the physical tests shown in Fig. 4, the simulation for the cases with the angled surface agrees less well with the forces measured in physical experiments. This indicates the difficulty of simulating the slipping phenomenon, and therefore the need for conducting physical experiments.

III. REDUCING OUT-OF-PLANE DEFORMATION

In the previous section, it has been demonstrated that a smaller out-of-plane deformation is beneficial for maintaining a firm contact with objects while under the same in-plane bending stiffness. Thus, it can potentially improve grasping stability. In the experiments, we increased the relative stiffness to out-of-plane deformation through an extra beam that

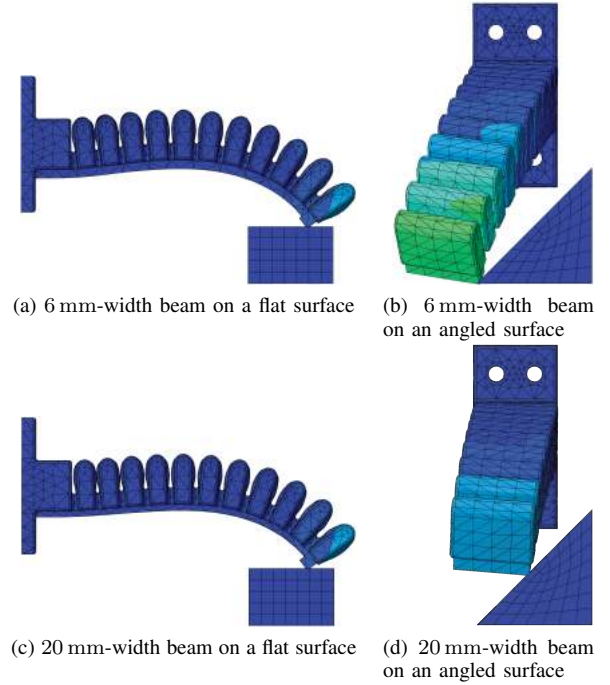


Fig. 7: Simulated deformation of the actuator with a 6 mm-width beam ((a) & (b)) and the one with a 20 mm-width beam ((c) & (d)). An obstacle with a flat surface ((a) & (c)) or an angled surface ((b) & (d)) is in the way of bending. The deformation results are similar in the case of a flat surface, while in the case of an angled surface the actuator with a 20 mm-width beam (d) shows a smaller sideways deformation.

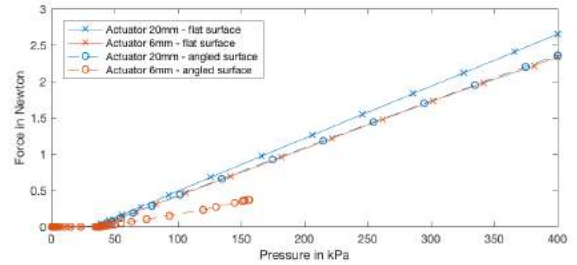


Fig. 8: Simulated vertical force between the actuators and the flat or angled surface.

was attached to the inextensible layer, which necessitates a higher actuation effort.

In this section, we present a newly designed stiffening-structure which has marginal effects on the in-plane bending but significantly increases the out-of-plane stiffness. The structure is shown in Fig. 9. The design is inspired by the infinity-flexure presented in [19]. We use the inextensible layer as the main flexure and add auxiliary flexures in perpendicular direction between each bellow segment. Then, the auxiliary flexures are connected at the ends through additional elements. Loading the actuator in torsion r_{x_l} will load the auxiliary flexures in the constrained r_{y_l} -direction (see Fig. 9). As the auxiliary flexures are connected in series,

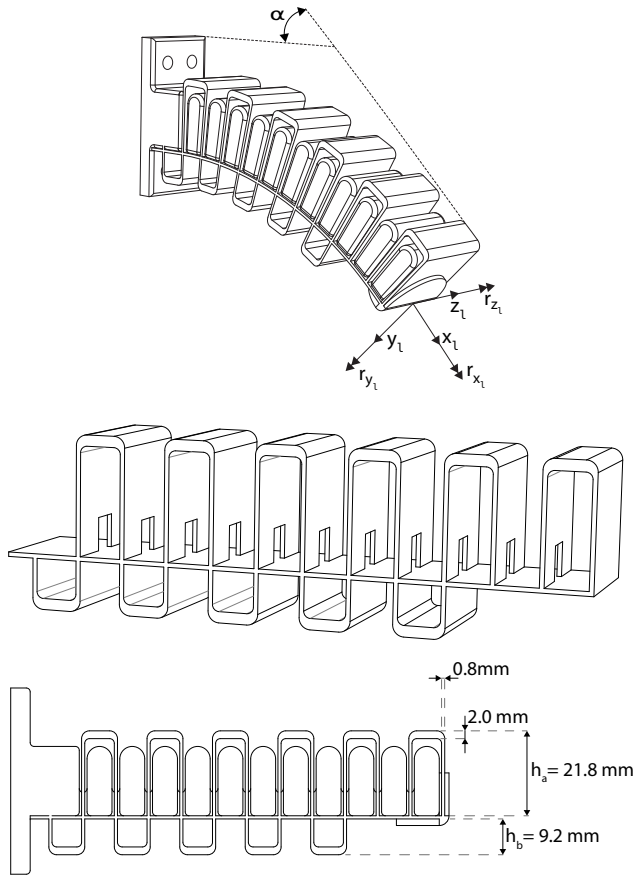


Fig. 9: The improved soft actuator design with stiffening structure.

their deflection angle is much smaller than the total deflection angle of the actuator α , thereby limiting the decrease of stiffness in r_{y_l} -direction. This ensures that the actuator retains a significant torsional stiffness at large deflection angles. At the same time, the auxiliary flexures barely increase the bending stiffness about the r_{z_l} -direction.

The heights of the auxiliary flexures above and below the inextensible layer are empirically determined and indicated in Fig. 9. A smaller height h_b increases the in-plane bending stiffness. However, a large h_b results in severe self-contact when the actuator bends forward. At the fingertip, no auxiliary flexures are added below, to avoid undesired interaction between the flexures and the grasping targets. We note that the upper auxiliary flexures are beneficial for forward bending. Collisions between the flexures and the expanding bellows effectively increase the elongation of the extensible layer, thus improving the bending performance [3]. On the other hand, these flexures reduce the range for reverse bending, which is sometimes required for grasping larger objects. In this case, the distance between the bellows should be increased.

IV. RESULTS

We compare our design to a reference design with an identical inextensible layer with a thickness of 0.8 mm and

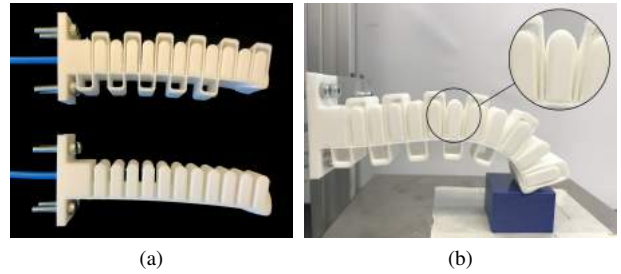


Fig. 10: (a) Fabricated design with and without stiffening structure. (b) Self-collision between the bellows and the stiffening-structure results in an increase in the exerted force.

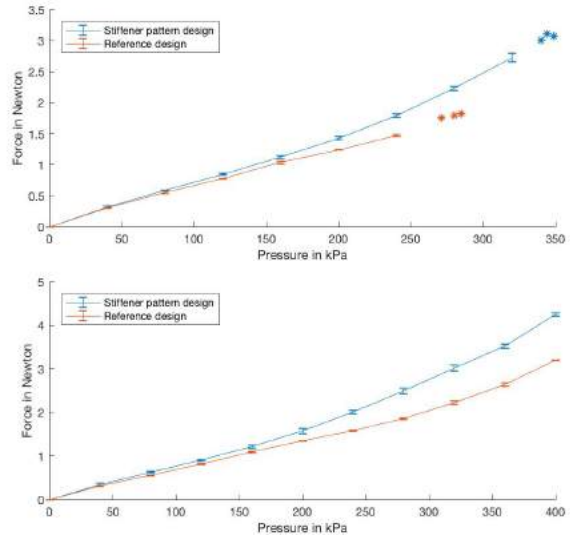


Fig. 11: Vertical component of the in-plane force exerted by different designs on a 45° angled surface (top) and a flat surface (bottom). Slippage points are indicated by a star.

a width of 20 mm (see the bottom of Fig. 10(a)). We test the actuators using the same setup shown in Fig. 3. Figure 11 shows the vertical forces exerted on the flat surface and the 45° angled surface. The design with stiffening-structure was able to exert a force of 3.11 N on a 45° angled surface before reaching a sideways displacement of 20 mm. This force is more than 70% higher than that of the reference design (1.82 N). It is also observed that at the same pressure the stiffening-structure reinforced design exerts a larger in-plane force on the flat surface. This can be explained by the accelerated self-collision between the bellows due to the stiffening-structure, as is highlighted in Fig. 10(b).

We integrate the bellows with stiffening-structure onto a gripper with three fingers. Figure 12 shows the newly designed gripper grasping a variety of objects stably at a pressure of 500 kPa. It should be noted that the gripper with the 6 mm-width beam failed to grasp the spherical object (Fig. 2) before reaching such a pressure, with a failure happening at a pressure of 400 kPa. Similarly, a gripper built from the reference design actuators (Fig. 10(b)) showed several failed grasps for the tape-measure, the wrench and

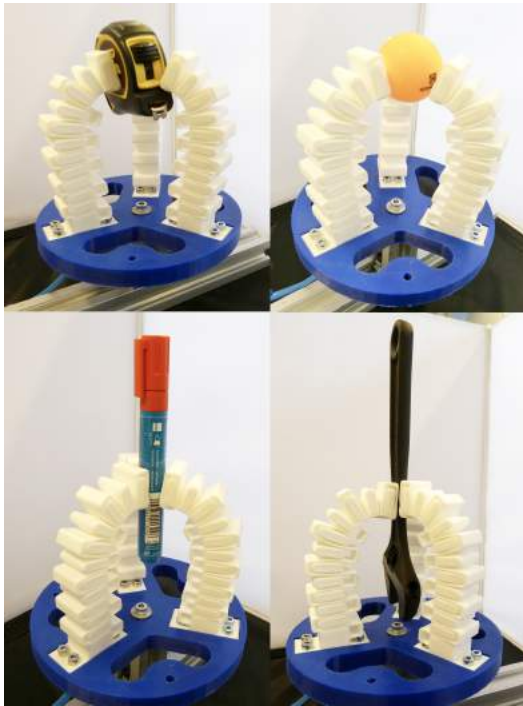


Fig. 12: A gripper consisting of three actuators with the stiffening-structure can stably grasp a variety of objects at a high pressure of 500 kPa.

the marker at pressures below 500 kPa due to out-of-plane deformation. The design with stiffening-structure also increases the quality of the successful grasps in terms of holding force. Note that oblong objects such as the wrench and the marker are held in place in a straight orientation, whereas the reference gripper would hold these objects in a less stable orientation due to out-of-plane deformation of the gripper fingers. We further demonstrate the improved grasping stability in the supplementary video material.

V. CONCLUSIONS

This paper demonstrates the importance of the out-of-plane stiffness of soft actuators for grasping stability. Under the same in-plane deformation, a smaller out-of-plane deformation is beneficial for stable grasping.

The newly designed stiffening-structure increases the out-of-plane stiffness with minimal influence on the in-plane stiffness. The stiffening-structure retains a significant out-of-plane stiffness when it is in a bent configuration. An actuator with the reinforced out-of-plane stiffness is able to exert higher forces without slippage when confronted with asymmetric loadings.

ACKNOWLEDGMENT

The authors wish to thank Prof. Just Herder at TU Delft for inspiring discussions on spatial flexures. The work is partially supported by CUHK Direct Research Grant (4055094).

REFERENCES

- [1] F. Iliovski, A. D. Mazzeo, R. F. Shepherd, X. Chen, and G. M. Whitesides, "Soft robotics for chemists," *Angewandte Chemie*, vol. 123, no. 8, pp. 1930–1935, 2011.
- [2] K. C. Galloway, K. P. Becker, B. Phillips, J. Kirby, S. Licht, D. Tchernov, R. J. Wood, and D. F. Gruber, "Soft robotic grippers for biological sampling on deep reefs," *Soft Robotics*, vol. 3, no. 1, pp. 23–33, 2016.
- [3] B. Mosadegh, P. Polygerinos, C. Keplinger, S. Wennstedt, R. F. Shepherd, U. Gupta, J. Shim, K. Bertoldi, C. J. Walsh, and G. M. Whitesides, "Pneumatic networks for soft robotics that actuate rapidly," *Advanced Functional Materials*, vol. 24, no. 15, pp. 2163–2170.
- [4] J. Hughes, U. Culha, F. Giardina, F. Guenther, A. Rosendo, and F. Iida, "Soft manipulators and grippers: A review," *Frontiers in Robotics and AI*, vol. 3, 2016, article 69.
- [5] T. Laliberte, L. Birglen, and C. Gosselin, "Underactuation in robotic grasping hands," *Machine Intelligence & Robotic Control*, vol. 4, no. 3, pp. 1–11, 2002.
- [6] T. Okada, "Computer control of multijointed finger system for precise object-handling," *IEEE Transactions on Systems, Man, and Cybernetics*, vol. 12, no. 3, pp. 289–299, May 1982.
- [7] S. Jacobsen, E. Iversen, D. Knutti, R. Johnson, and K. Biggers, "Design of the Utah/M.I.T. dextrous hand," in *Proceedings. 1986 IEEE International Conference on Robotics and Automation*, vol. 3, April 1986, pp. 1520–1532.
- [8] M. Rakić, "Multifingered robot hand with selfadaptability," *Robotics and Computer-Integrated Manufacturing*, vol. 5, no. 2, pp. 269 – 276, 1989.
- [9] K. Suzumori, S. Iikura, and H. Tanaka, "Development of flexible microactuator and its applications to robotic mechanisms," in *Proceedings. 1991 IEEE International Conference on Robotics and Automation*, vol. 2, April 1991, pp. 1622–1627.
- [10] R. Deimel and O. Brock, "A novel type of compliant and underactuated robotic hand for dexterous grasping," *The International Journal of Robotics Research*, vol. 35, no. 1-3, pp. 161–185, 2016.
- [11] V. Wall, G. Zller, and O. Brock, "A method for sensorizing soft actuators and its application to the RBO hand 2," in *2017 IEEE International Conference on Robotics and Automation (ICRA)*, May 2017, pp. 4965–4970.
- [12] J. Morrow, H. Shin, C. Phillips-Grafflin, S. Jang, J. Torrey, R. Larkins, S. Dang, Y. Park, and D. Berenson, "Improving soft pneumatic actuator fingers through integration of soft sensors, position and force control, and rigid fingernails," in *2016 IEEE International Conference on Robotics and Automation (ICRA)*, May 2016, pp. 5024–5031.
- [13] H. K. Yap, H. Y. Ng, and C.-H. Yeow, "High-force soft printable pneumatics for soft robotic applications," *Soft Robotics*, vol. 3, no. 3, pp. 144–158, 2016.
- [14] P. Polygerinos, S. Lyne, Z. Wang, L. F. Nicolini, B. Mosadegh, G. M. Whitesides, and C. J. Walsh, "Towards a soft pneumatic glove for hand rehabilitation," in *2013 IEEE/RSJ International Conference on Intelligent Robots and Systems*, Nov 2013, pp. 1512–1517.
- [15] P. Glick, S. A. Suresh, D. Ruffatto, M. Cutkosky, M. T. Tolley, and A. Parness, "A soft robotic gripper with gecko-inspired adhesive," *IEEE Robotics and Automation Letters*, vol. 3, no. 2, pp. 903–910, April 2018.
- [16] T. Yamada, T. Koishikura, Y. Mizuno, N. Mimura, and Y. Funahashi, "Stability analysis of 3d grasps by a multifingered hand," in *Proceedings 2001 ICRA. IEEE International Conference on Robotics and Automation*, vol. 3, May 2001, pp. 2466–2473 vol.3.
- [17] P. Polygerinos, Z. Wang, J. T. B. Overvelde, K. C. Galloway, R. J. Wood, K. Bertoldi, and C. J. Walsh, "Modeling of soft fiber-reinforced bending actuators," *IEEE Transactions on Robotics*, vol. 31, no. 3, pp. 778–789, June 2015.
- [18] D. M. Brouwer, J. P. Meijaard, and J. B. Jonker, "Elastic element showing low stiffness loss at large deflection," in *Proceedings of the 24th Annual Meeting of the American Society of Precision Engineering, Monterey, CA., 2009*, p. 3033.
- [19] D. H. Wiersma, S. E. Boer, R. G. K. M. Aarts, and D. M. Brouwer, "Design and Performance Optimization of Large Stroke Spatial Flexures," *Journal of Computational and Nonlinear Dynamics*, vol. 9, no. 1, pp. 11 010–11 016, nov 2013.
- [20] S. Awatar, A. H. Slocum, and E. Sevincer, "Characteristics of Beam-Based Flexure Modules," *Journal of Mechanical Design*, vol. 129, no. 6, pp. 625–639, may 2006.
- [21] W. C. Young, R. G. Budynas, and A. M. Sadegh, *Roark's formulas for stress and strain; 8th ed.* New York, NY: McGraw Hill, 2012.